Title: Mapping the soil microbiome functions shaping wetland methane emissions

Running title: Soil microbiome drivers of wetland methane emissions

Authors: Mikayla A. Borton[a+] (0000-0001-8037-4253), Angela M. Oliverio[a,b+] (0000-0002-0261-0393), Adrienne B. Narrowe[a] (0000-0002-2000-088X), Jorge A. Villa[c] (0000-0003-1130-9401), Christian Rinke[d] (0000-0003-4632-1187), David W. Hoyt[e] (0000-0002-2857-719X), Pengfei Liu[a,f] (0000-0003-1003-2025), Bridget B. McGivern[a] (0000-0001-9023-0018), Emily K. Bechtold[a] (0000-0001-5092-6264), Jared B. Ellenbogen[a] (0000-0003-1692-9044), Rebecca A. Daly[a] (0000-0003-2223-7458), Garrett J. Smith[g] (0000-0002-1014-5102), Jordan C. Angle[g] (0000-0002-3260-5851), Rory M. Flynn[a] (0000-0003-0709-2705), Andrew P. Freiburger[h] (0000-0002-7288-535X), Katherine B. Louie[i,j] (0000-0002-6787-7558), Brooke Stemple[a], Trent R. Northen[i,j] (0000-0001-8404-3259), Christopher Henry[h] (0000-0001-8058-9123), Christopher S. Miller[k] (0000-0002-9448-8144), Timothy H. Morin[l] (0000-0002-6504-6937), Gil Bohrer[m] (0000-0002-9209-9540), Kelly C. Wrighton[a*] (0000-0003-0434-4217)

[a] Department of Soil and Crop Sciences, Colorado State University, Fort Collins, CO, 80521
[b] Department of Biology, Syracuse University, Syracuse, NY, 13210
[c] School of Geosciences, University of Louisiana at Lafayette, Lafayette, LA 70503
[d] Department of Microbiology, University of Innsbruck, Innsbruck, Austria
[e] Environmental Molecular Sciences Laboratory, Pacific Northwest National Laboratory, Richland, WA, 99352
[f] Center for Pan-third Pole Environment, Lanzhou University, Lanzhou 730000, China
[g] Department of Microbiology, The Ohio State University, Columbus, OH 43210
[h] Data Science and Learning, Argonne National Laboratory, Lemont, IL 60439
[i] Lawrence Berkeley National Lab, Berkeley, CA, 94720
[j] DOE Joint Genome Institute, Lawrence Berkeley National Laboratory, Berkeley, CA, 94720
[k] Department of Integrative Biology, University of Colorado Denver, Denver, CO, 80217
[l] Department of Environmental Resources Engineering, State University of New York College of Environmental Sciences and Forestry, Syracuse, New York, 13210
[m] Department of Civil, Environmental & Geodetic Engineering, The Ohio State University, Columbus, OH, 43210

[+]**Authors contributed equally to this work:** Mikayla A. Borton and Angela M. Oliverio

[#]**Correspondence:** wrighton@colostate.edu

Keywords: genome, MAG, metagenomics, metatranscriptomics, global change, greenhouse gases, methanogen

Abstract: Accounting for only 8% of Earth's land coverage, freshwater wetlands remain the foremost contributor to global methane emissions. Yet the microorganisms and processes underlying methane emissions from wetland soils remain poorly understood. Over a five-year period, we surveyed the microbial membership and in situ methane measurements from over 700 samples in one of the most prolific methane-emitting wetlands in the United States. We constructed a catalog of 2,502 metagenome-assembled genomes (MAGs), with more than half of the 70 bacterial and archaeal phyla sampled containing novel lineages. Integration of these data with 133 soil metatranscriptomes provided a genome-resolved view of the biogeochemical specialization and versatility expressed over wetland soil spatial and temporal gradients. Centimeter-scale depth differences best explained patterns of microbial community structure and transcribed functionalities, even more so than land coverage or temporal information. Moreover, while extended flooding restructured soil redox, this perturbation failed to reconfigure the transcriptional profiles of methane cycling microorganisms, contrasting with theoretical expected responses to hydrological perturbations. Co-expression analyses coupled to depth resolved methane measurements exposed the metabolisms and trophic structures most predictive of methane hotspots. Mapping the spatiotemporal transcriptional patterns on this compendium of biogeochemically classified soil derived genomes begins to untangle the microbial carbon, energy, and nutrient processing contributing to wetland methane production.

Importance: Soil microbial ecology is increasingly recognized as essential to climate mitigation, but realizing its full potential requires shifting from static genome inventories to dynamic assessments of microbial activity. This study shows that methane-cycling microbes exhibit stable, depth-stratified expression patterns, even in response to major redox and flooding shifts,

undermining assumptions that water-table manipulations common in wetland management can alone reduce methanogenesis. Instead, methane cycling is shaped by spatially organized, transcriptionally active networks involving not only methanogens but also methanotrophs, fermenters, and iron reducers. These findings expose the limitations of genome-only models and highlight the need for soil diagnostics that capture in situ activity. Together, we provide a foundation for developing activity-based microbiome tools, embedding microbial functions into Earth system models, and designing interventions that move beyond “single lever” strategies and instead work with the structure and dynamics of microbial communities as complex, layered systems.

Introduction

Wetlands are characterized as waterlogged soils, rich in organic matter, with low concentrations of oxygen in the porewater. Consequently, the anoxic microbial decomposition of this soil organic matter leads to the production of biogenic methane (CH_4). As such, wetland soils are the largest and most variable source of this potent greenhouse gas, accounting for nearly a third of annual CH_4 emissions (1–4). Despite this global climate relevance, the microbial communities and metabolic pathways driving the conversion of soil organic carbon to CH_4, along with their environmental controls, remain unresolved. This knowledge gap hinders the incorporation of microbial processes into land surface and biogeochemical models, impeding the accurate management and predictions of greenhouse gas (GHG) fluxes from wetlands (3, 5, 6).

Over the last decade, metagenomic sequencing approaches have described the microbial community membership and function associated with CH_4 production across a range of habitats. While other high CH_4 emitting systems, like wastewater (7), ruminants (8), or subsurface (9), habitats have received considerable genomic scrutiny, wetland soils remain relatively underexplored in terms of microbial genomic sampling. Of the handful of genome-resolved studies from freshwater wetlands, nearly all are focused on organic soils from northern peatlands (10–13). One notable study, from thawing permafrost in Sweden, yielded ~1,500 metagenome assembled genomes (MAGs) (11), serving as the stand alone microbial catalog for all wetland soils. This means the highest CH_4-contributing wetland types, temperate and tropical marshes, have only a few genome-resolved studies to date (14–16). These studies emphasized the roles of a limited number of microorganisms to specific biogeochemical processes (14–17), such as methanotrophy, yet failed to inventory the overall composition, function, and interconnected metabolic pathways driving CH_4 production across diverse wetland gradients.

101 To bridge this knowledge gap, we undertook a comprehensive sampling within a
102 temperate freshwater marsh, aiming to elucidate the spatiotemporal related variations in the
103 microbiome. This freshwater wetland was chosen due to its exceptionally high CH_4 fluxes,
104 exceeding ten times the median flux observed in wetlands with similar annual temperature
105 ranges (18, 19), and because of its susceptibility to climate-induced flooding events influenced
106 by fluctuating Lake Erie water levels (20). Leveraging more than 5 Tera basepairs of sequencing,
107 we reconstructed thousands of microbial genomes and integrated this data with soil
108 metatranscriptomes, geochemistry, and greenhouse gas porewater measurements and fluxes.
109 Here we delineate the expressed membership and metabolisms of the microbial community,
110 shedding light on the biogeochemical contributions of hundreds of understudied lineages. These
111 findings offer new perspectives on the stability and interactions of metabolic guilds driving CH_4
112 production in temperate, freshwater wetland ecosystems. This study provides mechanistic
113 insights that pave the way for activity-based methane mitigation strategies and more accurate
114 integration of microbial processes into Earth system models (21).
115

116 **Results**

117 **Sampling microorganisms from wetland soils**

118 As a model wetland we selected the highest methane-emitting wetland in the AmeriFlux
119 network (site ID US-OWC), an investigator network with tailored instrumentation, data
120 processing, and standardized procedures for flux measurements (19, 22–24). The Old Woman
121 Creek (OWC) wetland was instrumented to measure wetland CH_4 at various spatiotemporal
122 scales (**Supplementary Fig. 1**), facilitating a detailed assessment of the microbial processes that
123 impact soil CH_4 dynamics. Based on land coverage types, we parsed the wetland into 10 patches

124 (**Fig. 1A**). These patches included 5 land coverage types including emergent vegetation-*Typha*
125 (n=1), emergent vegetation-*Nelumbo* (n=3), standing freshwater or open water (n=3), and
126 temporal mud flats (n=3). From selected sites, once per month during sampling campaigns,
127 dialysis peepers measured soil CO_2 and CH_4 concentrations along ~3cm-depth increments up to
128 30 cm deep. This content was paired to surface chamber flux measurements for CO_2 and CH_4
129 and site wide fluxes using the eddy covariance and meteorological station. Surrounding the
130 peepers, soil cores were pulled and extruded at 5 cm depth increments down to 25 cm to result in
131 705 samples for soil geochemical, metabolite, and microbial analysis. In summary, across the
132 five-year sampling campaign (2013-2018), each one of these 10 ecological patch sites was
133 sampled at least 52 times for paired microbial, soil geochemistry, flux and porewater GHGs. The
134 inventory of measured geochemistry and flux data and their relationships is shown in
135 **Supplementary Fig. S2**.
136 We screened 671 of these collected soil samples with 16S rRNA amplicon sequencing for
137 methanogen membership (**Supplementary Table S2**), identifying 42 samples for deep
138 metagenomic sequencing (**Supplementary Table S1**). We generated up to 300 Gbp of
139 sequencing per sample, resulting in 3.1 Tbp total metagenomic sequencing (**Supplementary**
140 **Table S3**). Collectively, this effort doubled the amount of metagenomic sequencing from
141 wetland soils available in public repositories (**Supplementary Fig. 1D**). Given that one of our
142 primary objectives was to increase the recovery of methanogen genomes from soils, multiple
143 assembly and binning methods targeted the recovery of these lineages (**Supplementary Fig. 1E**).
144 This approach resulted in over 17,333 draft genomes, which were dereplicated into a final
145 collection of 3,217 genomic representatives, with 2,502 of these constituting high and medium
146 quality metagenome assembled genomes (MAGs) (**Supplementary Fig. S1**).

147 To map which microbial genomes recruited transcripts and which metabolisms were
148 expressed across sites, depths, seasons, and years, we obtained 2.7 Tbp of metatranscriptome
149 sequencing from 133 soil samples. Nearly 80% of the metatranscriptomes had paired NMR
150 detected metabolites to profile methanogenic substrates across the sample set (**Supplementary**
151 **Table S4**). This comprehensive multi-omics sampling across wetland gradients, including
152 multiple land coverage types, depths, and times, provides the first insights into the microbial
153 structural and functional diversity residing in temperate freshwater wetland soils.
154

155 **Uncovering thousands of transcribed genomes from wetland soils**

156 We reconstructed MAGs from 60 bacterial (N=2,204 MAGs) and 10 archaeal (n=298
157 MAGs) phyla that included 85 methanogen-related MAG representatives. Many MAGs
158 recovered here were designated newly sampled lineages at the genus level or higher including
159 genome representatives with unnamed classes (n=4 MAGs), orders (n=20 MAGs), families
160 (n=15 MAGs), and genera (n=122 MAGs) (**Supplementary Table S3**). In addition, hundreds of
161 genomes were from poorly or previously uncharacterized phyla often denoted only by an
162 alphanumeric identifier or placeholder name, such as QNDG01, CSP1-3, and KSB1 (**Fig. 1B**). In
163 this wetland, the most represented phyla are the archaeal Halobacteriota (n=74 MAGs) and the
164 bacterial Pseudomonadota (n=484, formerly Proteobacteria), Acidobacteriota (n=316 MAGs),
165 Desulfobacterota (n=252), and Chloroflexota (n=237 MAGs). The reconstruction of these
166 thousands of genomes, many metabolically uncharacterized, highlights the vast, unsampled
167 microbial diversity still residing within soils.

168 Approximately 75% of the reconstructed genomes (n=1948) recruited transcripts from the
169 133 metatranscriptomes. We report the maximum transcription for each MAG and denote the top

170 12 most transcriptionally dominant MAGs from each bacterial or archaeal domain (**Fig. 1BC**).
171 These MAGs with dominant transcription also have high transcriptional occupancy, with a
172 minimum detection in 35% across the 133 metatranscriptome samples (**Fig. 1C).** A significant
173 majority (83%) of these transcriptionally dominant genomes belong to poorly characterized
174 genera as noted by their names (e.g., genera defined only by alphanumeric code). The prevalence
175 of transcriptionally dominant but poorly classified genomes reveals a gap in our understanding of
176 the organisms actively shaping wetland biogeochemistry.
177
178 **Connecting transcribed biogeochemical functions to microbial taxonomy**
179 Each of the 1,948 MAGs that recruited transcripts was assessed for expressed gene
180 content relating to 14 biogeochemical processes: oxygen (aerobic respiration, microaerophilic
181 respiration), methane (methanogenesis, aerobic methanotrophy, anaerobic methanotrophy),
182 sulfur (sulfur oxidization, sulfur reduction), nitrogen (nitrification, nitrogen reducer, nitrogen
183 fixation, and Dissimilatory Nitrate Reduction to Ammonium (DNRA)), iron (iron oxidation, iron
184 reduction), and other metabolisms (phototrophy, obligate fermentation) (**Supplementary Fig.
185 S3, Methods**). This resulted in 1,135 MAGs that contained sufficient gene transcript recruitment
186 to be assigned to at least one of these 14 biogeochemical guilds (**Supplementary Table S5)**.
187 Aerobic and microaerophilic metabolisms were the most widely encoded across wetland
188 lineages (**Fig. 2A**). We compared the dominant encoded metabolic traits (i.e., detected in the
189 greatest number of genomes) to the most dominant transcribed traits, finding the transcribed
190 functionalities did not follow the encoded (**Fig. 2B**). For example, the capacity for
191 microaerophilic and aerobic respiration was detected in the largest percentage of genomes (53%
192 and 51%) but only detected in 8% and 6% of genomes in our transcriptomes respectively. In

193 contrast, transcription for genes enabling anaerobic metabolisms like obligate fermentation, iron
194 reduction, and nitrogen reduction were detected more so than aerobic metabolisms. This
195 enrichment for anaerobic metabolisms in the transcript signal is not entirely surprising given that
196 most soils in our data set have pore-water dissolved oxygen (DO) concentrations below the 1uM
197 detection limit (**Supplementary Table S4**). Our approach reveals that transcriptional profiles
198 capture environmentally responsive metabolic activity not evident from genome content alone,
199 underscoring the importance of expression-based profiling to uncover active microbial processes.
200 Focusing on transcribed functions, at the phylum level we found that certain phyla, such
201 as Thermoproteota or Halobacteriota, are characterized by a pink or purple color, indicating their
202 specialization as obligate fermenters or methanogens (**Fig. 2C**). In contrast, phyla like the
203 Pseudomonadota and Acidobacteriota exhibit a wide array of colors, signifying their trait
204 multifunctionality at the phylum level. This analysis also reveals disproportional contributions
205 from phyla to nutrient and redox transformations. For instance, MAGs transcribing genes for
206 sulfur reduction are enriched in the Desulfobacterota, iron reduction are prevalent in the
207 Acidobacteriota and Nitrospirota, aerobic respiration are prevalent across the Chloroflexota, and
208 nitrogen reduction and sulfur oxidation are enriched in some lineages of the Pseudomonadota.
209 Notably, keystone processes like nitrification and nitrogen fixation were both rare (<5% of
210 MAGs) and phylogenetically dispersed (**Supplementary Table S5**). Nitrogen fixation, for
211 example, was detected in transcripts from just nine MAGs across three phyla that encompassed
212 aerobes, iron reducers, and denitrifiers, as well as a methanogen and a nitrifier, illustrating how
213 assimilatory and dissimilatory processes are coupled. This trait mapping reveals the phylogenetic
214 distribution of key metabolic activities and underscores the diverse, active roles that
215 microorganisms play in driving nutrient and redox transformations.

Identifying the dominant drivers shaping wetland microbiome structure and function

The relative expression of genomes across depth profiles revealed distinct microbial community structures in the Plant, Mud, and Open Water habitats (**Figure 3**). In Plant habitats, Pseudomonadota dominated the surface layers (0–5 cm), while deeper layers (15–25 cm) showed an increased abundance of Desulfobacterota and Bacteroidota; similar phyla were present in Mud habitats, but Desulfobacterota was more consistently abundant throughout the profile, with Verrucomicrobiota becoming more pronounced at depth. In Open Water habitats, Pseudomonadota were again prominent near the surface, but deeper layers shifted towards Gemmatimonadota and Thermoplasmatota, suggesting increased anaerobic processes with depth. These patterns reflect habitat differences in microbial activity and adaptation along the redox gradient within each environment.

To test how different wetland environments influenced the soil microbiome, we evaluated the impact of 17 spatial, temporal, and geochemical factors across three levels of biological organization: (i) phylotype membership, (ii) transcriptionally 'active' genome membership, and (iii) expressed functional guilds (**Fig. 3BC**). Our analyses revealed that, regardless of the microbiome attribute measured, depth and depth-related geochemistry (such as soil Fe (II) and cation exchange capacity, CEC) were the best predictors of wetland soil microbiome structure and function, more so than differences from the different land coverages. These chemical and physical soil attributes played a more direct role in shaping expressed functional guilds, explaining 40 to 50% of this variation, nearly double variation explained for the phylotype data (**Supplementary Fig. S4**). Overall, this information can inform wetland microbiome sampling priorities, showing the value of adding more depth-resolved measurements and affirming

239 collection of high-priority geochemical variables, such as CEC, Fe (II), pH, and acetate, while
240 also recognizing that porewater oxygen measurements using hand held probes may fail to resolve
241 redox microsite heterogeneity that drives wetland biogeochemical activity (15).
242
243 **Uncovering newly defined archaeal roles in carbon cycling**
244 A valuable component of our sampling was the broad recovery of archaeal genomes
245 (n=298 MAGs), spanning 10 phyla with 48 families including 88 genera. When considering the
246 functional roles of Archaea in wetlands, these microorganisms were historically regarded
247 primarily as methanogens or metabolizing other single carbon (C1) compounds (16, 25–27).
248 Here we derived a gene-based rule set to assign these genomes to carbon decomposition guilds
249 of (i) polymer hydrolysis, (ii) sugar oxidation, (iii) organic acids and nitrogen conversions, and
250 (iv) C1 metabolisms (**Supplementary Table S7**).
251 We show phylogenetically diverse archaeal lineages expressed genes for hydrolyzing
252 these plant polymeric constituents **(Fig. 4)**. Depolymerization results in the second trophic group,
253 yielding sugars and other oligomers or monomers. Lineages like Thorarchaeaceae and UBA233
254 transcribed genes to use 6 or more substrates that span both polymeric and sugar trophic groups.
255 We also identified sugar utilizing specialist archaea (e.g., members of the TCS64) that expressed
256 genes for utilizing at least 3 sugar substrates. In support of these expressed sugar metabolisms,
257 raffinose, sucrose, and maltose like compounds were prevalent across the metabolome data
258 (**Supplementary Table S8-S9**), giving further credence to the likelihood of these metabolisms in
259 situ. These findings provide evidence that Archaea, often overlooked in primary carbon
260 degradation, contribute far more broadly to soil carbon turnover than previously recognized,
261 occupying roles across multiple carbon trophic levels.

262 The third guild before methane production yields small molecular weight compounds like
263 organic acids (e.g., acetate, butyrate, lactate) and methylated (e.g., methylamine, methanol)
264 compounds. Some of these are methanogenic substrates, while others can be further fermented,
265 typically syntrophically, to yield methanogenic substrates. This latter guild had the greatest
266 transcriptional prevalence across the archaeal genomes, indicating the critical role these archaea,
267 most of them diagnosed as obligate fermenters, could play in cross feeding methanogens.
268 The fourth guild of carbon is C1 metabolisms, with nearly a third of the archaeal
269 genomes assigned as methanogens, representing 4 phyla (Methanobacteriota, Thermoproteota,
270 Halobacteriota, Thermoplasmatota). The 85 methanogen MAGs spanned 10 families with 20
271 genera, 8 of the latter were new genera first identified here (**Supplementary Fig. S5**). Beyond
272 canonical methanogens, we also recovered genomes from presumed non-methanogenic, *mcrA*-
273 containing taxa such as the anaerobic methanotrophic *Methanoperedens* genus and the alkane-
274 oxidizing Helarchaeales. Prior to this effort, the largest wetland MAG database contained 21
275 methanogen representatives with 4-fold less genus level diversity (11). Despite their direct
276 climate feedback role, it is astonishing that multiple new, highly active methanogens can still be
277 recovered from a single wetland.
278 Beyond taxonomic novelty, metabolic reconstruction with paired transcriptional profiles
279 offered new insights into wetland methanogenesis (**Supplementary Fig. S5**). Acetoclastic
280 methanogenesis was confined exclusively to *Methanothrix* and closely related members (16
281 MAGs). Our field data reinforce laboratory studies of *Methanothrix* and *Methanosarcina* (28),
282 indicating that obligate acetoclastic *Methanothrix* outcompetes the facultative acetoclast
283 *Methanosarcina* in situ due to more efficient substrate acquisition under the low acetate
284 concentrations typical of these wetland soils (mean 45 μM; **Supplementary Fig. S6**). Across the

285 methanogens, obligate hydrogenotrophy was the most prevalently transcribed pathway in 52% of
286 the MAGs, with two of the most transcriptionally active Archaea identified as obligate
287 hydrogenotrophs (*Methanoregula* and UBA9949, **Fig.1**). This work confirms and extends
288 canonical methanogenic paradigms by showing not just potential but active dominance of
289 *Methanothrix* and *Methanoregula* under natural, low-substrate field conditions.
290 While wetland CH_4 is commonly attributed to acetoclastic and hydrogenotrophic
291 methanogens (3), our findings highlight the overlooked importance of methylotrophic pathways.
292 We found that 25% of wetland methanogen MAGs expressed genes for methylotrophic
293 methanogenesis and one of the most transcriptionally active Archaea, *Methanomethylicus*, was a
294 methylotroph (**Fig. 1C**). Additionally, we detected methylotrophic gene expression in lineages
295 traditionally considered hydrogenotrophic, including *Methanoregula* MAG and in one MAG
296 belonging to a novel genus within the *Methanospirillaceae* family (**Supplementary Fig. S5**). We
297 further resolved substrate preferences for methylotrophic methanogens, showing specificity for
298 methylated nitrogen, sulfur, and oxygen compounds. Supporting this, NMR and LC-MS analyses
299 frequently detected methyl-N compounds (e.g., betaine, carnitine) and methyl-O compounds
300 (e.g., methanol, vanillic acid) at higher concentrations and in more samples than canonical
301 substrates like formate or acetate (**Supplementary Fig. S6**). These findings reinforce an
302 emerging consensus that methylotrophic methanogenesis may be a widespread and
303 underappreciated source of methane in wetland ecosystems (16, 27, 29).
304
305 **Methane cycling guilds are temporally stable along a depth gradient over years**
306 Methane cycling genome-based transcription patterns from a flooded mud-flat collected
307 monthly over a 3-month summer 2018 season exposed methanogen and methanotroph

308 spatiotemporal niches and possible depth-defined ecotypes (**Supplementary Fig. S7**). We
309 uncovered six core methanogens, from diverse functional and phylogenetic backgrounds, with
310 high levels of mean transcription across all soil depths and timepoints. The remaining CH_4
311 cycling members were localized to specific soil depths, forming co-expressing clades that
312 persisted across this summer season. We report a greater proportional enrichment of acetoclastic
313 and aerobic methanotrophs in surface soils, while the middle and deepest soil layers included the
314 anaerobic methane-oxidizing *Methanoperedens* genome and proportionally more
315 hydrogenotrophic and methyl-utilizing methanogens. Reflecting these latter methanogens
316 requirements for hydrogen, we observed increased formate concentrations from deeper (10-30
317 cm) depths across our mud, plant, and open water land coverage patch types (**Supplementary**
318 **Fig. S6**). Our findings highlight the persistence of depth-stratified methane 'neighborhoods',
319 composed of many closely related strains with a high-degree of functional redundancy.
320 Given the seasonal stability across summer 2018, we next compared the multi-omics data
321 collected from this site in August 2018 to parallel samples from the same mud flat in August
322 2015. During this time, the wetland flooded and the exposed mudflat from 2015 was beneath 5.3
323 ft of overlying freshwater in 2018. Based on existing theory about the redox sensitivity of
324 methanogens and their responses to hydrological perturbations (30), with flooding we
325 hypothesized to observe decreased dissolved oxygen (DO) concentrations and increased
326 methanogen expression broadly across the community, particularly in surface soils. Matching
327 flooding expectations, DO decreased to non-detectable levels in surface soils subsequent to
328 flooding. In contrast to expectations, 90% of the methanogen and aerobic methanotroph
329 (Methylococcaceae, Methylomonadaceae) MAGs experienced no significant change in mean
330 genome transcription in the flooding restructured surface soils (**Fig. 5)**. Worth noting, a few taxa

331 were flooding-responsive, like the methylotrophic *Methanomethylicus* (**Fig. 1C**). Supporting this
332 lack of restructuring in the CH_4 cycling microbiome, the concentrations of methanogenic
333 substrates like formate, methanol, and acetate did not change with flooding (**Supplementary**
334 **Fig. S6**). This flooding response may be due to the fact that methanogens in these routinely
335 submerged and drained soils surface soils could be already sheltered within anoxic microsites,
336 such as biofilms or soil aggregates (15, 31).
337
338 **Co-expression networks reveal key lineages modulating soil greenhouse gasses**
339 We implemented a workflow to integrate the data collected across this manuscript to
340 render the carbon and energy trophic network predictive of soil CH_4 concentrations
341 (**Supplementary Fig. S8**). First, weighted gene co-expression identified 7 modules composed of
342 genomes with shared transcriptional patterns across our 133 metatranscriptome samples (**Fig.**
343 **6A**). Two of these modules predicted soil porewater CH_4 concentrations, with the surface-soil
344 associated turquoise module negatively correlated and the deeper-soil associated brown module
345 positively correlated to soil CH_4 concentrations (**Fig. 6A**). These surface and deep modules
346 contained 551 and 372 MAGs, respectively. The top ten microbial genomes with the greatest
347 importance for CH_4 prediction and their transcribed biogeochemical traits are also noted (**Fig.**
348 **6CD**). Distilling the transcribed carbon and energy functional gene content of these predictive
349 genera, we mapped the trophic configurations that contribute to CH_4 concentrations in these
350 depth-defined compartments (**Fig. 6E**).
351 Consistent with our taxonomic-based analyses, we found key biogeochemical processes
352 (such as iron reduction, microaerophilic respiration, and methane production) were transcribed
353 across depths in these predictive modules (**Fig. 6CD**). The iron-reducing Zikibacteria and the

354 obligate fermenter Syntrophales were important predictors in both depth compartments
355 However, distinct microbial lineages were often responsible for mediating the same functions at
356 different depths. For instance, microaerophilic respiration involved *Bacteroidales* in surface
357 soils, while *Anaerolineales* and *Sedimentisphaerales* fulfilled similar roles in deeper soils. The
358 turquoise surface module also included functions not observed in the deep module, such as
359 nitrate reduction and low-affinity cytochrome oxidase expression, traits adapted to higher oxygen
360 conditions. Additionally, transcriptional evidence for aerobic methanotrophy (*Methylococcaceae*
361 UBA6136 and *Methylomonadaceae* KS41) was exclusive to the surface module. This likely
362 explains the negative correlation between the turquoise module and CH_4 concentrations in
363 surface soils (**Fig. 6B**).
364 Together, these transcriptome-derived, process-based observations reveal expressed
365 biogeochemical interactions in wetland soils. Soil CH_4 concentrations appear to be emergent
366 properties of the microbiome, driven not by individual methanogens alone, but by complex,
367 depth-resolved interactions among microbial guilds. Notably, the strongest predictors of soil
368 porewater CH_4 concentrations were often upstream carbon-oxidizing organisms such as iron
369 reducers (*Zikibacteria, Eisenbacteria, Geomobilibacter*) and fermenters (*Aminicenantales*) that
370 likely support diverse functional methanogens (*Methanoregula, Methanothrix,*
371 *Methanomethylicus*). These findings underscore the need for higher-throughput tools to resolve
372 microbial interactions in the context of ecosystem-scale methane dynamics.
373

374 **Discussion**

375 **Depth-structured microbiomes and redundancy shape wetland stability**

376 Our study reveals that depth is the dominant axis structuring microbial composition and
377 transcriptional activity in freshwater wetland soils. Across spatial and temporal gradients,
378 microbial communities and biogeochemical functions were vertically stratified, with functional
379 guilds consistently aligned with depth-defined redox and geochemical profiles. Traits such as
380 methanogenesis, iron reduction, and fermentation were expressed by phylogenetically diverse
381 organisms within the same depth layers, indicating high transcriptional redundancy. This
382 redundancy, both within and across lineages, likely buffers methane-cycling functions against
383 environmental fluctuations and contributes to the long-term stability of CH_4 production. While
384 previous inferences of functional redundancy were drawn from alpha diversity or genome-level
385 data (32), our findings demonstrate this redundancy at the level of gene expression and
386 functional traits, offering mechanistic evidence of activity-based ecosystem resilience.
387 Contrary to the microbial seed bank hypothesis (33), we observed widespread
388 transcriptional activity across archaeal and bacterial genomes. Specifically, 78% of the 2,502
389 genomes recruited transcripts, with 60% of these MAGs expressing sufficient genome content to
390 permit metabolic assignments to 14 traits associated with wetland biogeochemistry. Moreover,
391 the average MAG mean transcriptional occupancy was 59%, signifying active members were
392 maintained across samples that span diverse wetland gradients. These patterns suggest that,
393 rather than lying dormant, a large fraction of the wetland microbiome is metabolically active and
394 responsive across depth and time. While functional redundancy may provide ecological
395 resilience, it also complicates methane mitigation. In highly redundant systems, inhibiting one
396 lineage or process may simply lead to functional compensation by others, a microbial game of
397 'whack-a-mole'. As such, successful mitigation strategies must move beyond single-target

interventions and account for the depth-resolved, community-level architecture of soil microbiomes.

Expanding the methane paradigm: beyond classical substrates and lineages

This study also expands the framework of methane cycling by identifying alternative metabolic routes and underappreciated contributors. Although acetoclastic and hydrogenotrophic methanogenesis dominate conventional models (34), nearly a quarter of transcriptionally active methanogens in our study expressed genes for methylated compound utilization. These findings suggest that CH_4 production is not just fueled by acetate or hydrogen but also by methylated nitrogen, sulfur, and oxygen-containing substrates. Moreover, methane concentrations in porewater were more accurately predicted by co-expression networks involving iron reducers, obligate fermenters, methane oxidizers, and microaerophilic heterotrophs than by methanogens alone. These data reveal methane as an emergent property of integrated, depth-specific microbial consortia. In surface soils, aerobic methanotrophs likely attenuate CH_4 as its produced (based on the strong spatial co-expression), while deeper modules are dominated by organisms facilitating substrate production and syntrophic hydrogen production (**Fig. 6**).

These findings reinforce the need for methane mitigation strategies that are not only taxon-specific but also spatially and functionally informed. Interventions that ignore the trophic structure and spatial organization of microbial communities risk being ineffective or short-lived. For example, in other methanogenic systems such as the rumen (35, 36), mitigation approaches increasingly target upstream methanogen metabolic partners, manipulating redox conditions, or rerouting electron flow to non-methanogenic microbes. Similarly, recent work has shown that catechin, a naturally occurring plant metabolite found in wetland soil microbiomes, can suppress

methane production by up to 84% by redirecting hydrogen flux away from methanogens (37). Especially in complex environments like saturated soils, precision strategies that consider microbial interdependencies, metabolic plasticity, and depth-resolved activity are likely to offer more robust and scalable outcomes for methane mitigation.

Implications for redox-informed Earth system models

Our genome-resolved transcriptional profiles reveal seasonal and multi-year stability in methane-cycling activity across soil depths, despite substantial hydrological and redox perturbations. While we previously reported elevated CH_4 production under oxygenated conditions at this site in 2015 (15), new flooding data reinforce that methanogen transcription is largely unresponsive to shifts in soil oxygen concentrations. These findings add to a growing body of evidence challenging the long-standing paradigm that oxygen is the primary regulator of wetland CH_4 production (32–35). In our data, methanogen transcripts persisted in surface soils with detectable oxygen and showed no significant change following a 5.3-foot flood-induced redox shift, while aerobic methanotrophs remained active even under anoxic conditions. This decoupling suggests that microbial populations may be insulated within anoxic microsites, such as aggregates or biofilms, buffering them from bulk redox conditions. These results expose the limitations of using coarse redox proxies like dissolved oxygen in Earth system models and underscore the need for finer-scale, spatially explicit observations to resolve methane-cycling heterogeneity in wetlands.

Current biogeochemical models also largely neglect methylotrophic methanogenesis, despite mounting evidence that transcriptionally active methanogens frequently utilize methylated nitrogen-, sulfur-, and oxygen-containing compounds (16, 27, 38–40). These

substrates, which we show are abundant in situ, may represent a substantial and previously under-accounted source of CH_4 emissions. To incorporate these pathways into predictive frameworks, targeted cultivation of methyl-reducing methanogens is needed (39, 41), particularly from wetland environments where cultured representatives remain scarce. Such efforts are essential for generating key physiological parameters (e.g., uptake kinetics, growth optima, yields), paralleling existing knowledge for acetate- and hydrogen-utilizing methanogens. In parallel, stable isotope-based approaches will be vital for tracing substrate fate and quantifying the relative contribution of methylotrophy to CH_4 emissions. To help focus these efforts, our transcriptomic analysis distilled 85 methanogens into a "most wanted" list of four genera (*Methanoregula*, *Methanothrix*, *Methanomethylicus*, and Methanospirillaceae UBA9949) based on their transcriptional activity and predictive value for CH_4 concentrations (**Fig. 1, Fig. 6**). Supporting this prioritization, a recent cross-site comparison across nine temperate wetlands (29), including Old Woman Creek, found *Methanoregula* and *Methanothrix* to be core taxa, with *Methanoregula* consistently emerging as a network hub strongly predictive of CH_4 flux. As methane remains a powerful lever for near-term climate mitigation (42), advancing the biochemical and ecological understanding of these keystone methanogens, and the environmental controls shaping their activity, is paramount for improving process-based models and enabling targeted interventions across wetland ecosystems.

Accurately predicting methane flux in wetlands requires a shift toward models that capture the functional and spatial organization of microbial communities. Recent advances, such as the genome-to-ecosystem framework, have shown that incorporating genome-inferred biogeochemical traits weighted by community composition can markedly improve methane predictions in peatlands, reducing model bias by more than 50% (43). While impactful, these

467 models rely solely on genomic potential, which our findings suggest may fail to capture the
468 biogeochemical pathways actively driving emissions. Our work builds on and extends this
469 approach by integrating metatranscriptomic data to define trophic modules that reveal depth-
470 stratified networks of carbon oxidizers, syntrophic cross-feeders, terminal methanogens, and
471 methane oxidizers. By identifying the most active and predictive processes, our findings provide
472 a foundation for developing in situ diagnostics that move beyond multi-omic sampling toward
473 cost-effective proxies of microbial function. Embedding activity-based functional traits into
474 Earth system models will be critical for improving methane predictions and informing scalable,
475 precision-guided interventions across diverse wetland ecosystems.
476
477 **Conclusion**
478 In this study, we employed a comprehensive, multi-omics survey of wetland soils to
479 generate an unprecedented view of the structural and functional microbiome attributes that
480 underpin biogeochemical cycling. This approach helps move soil microbiome research beyond
481 the historical "black box" of environmental inputs and outputs, revealing how microbial
482 community composition and gene expression respond to depth and geochemical gradients. To
483 interpret this complexity, we developed gene-based rules to classify microbial energy
484 metabolisms and carbon trophic guilds, enabling us to resolve emergent properties of methane-
485 cycling consortia. This framework uncovered previously unrecognized roles for archaeal
486 lineages in carbon decomposition, revealed the substrate versatility and redox resilience of
487 methanogens, and demonstrated stable, depth-stratified co-expression patterns predictive of soil
488 CH_4 concentrations. Together, these insights provide a mechanistic foundation for embedding

microbial activity into Earth system models and for guiding microbiome-informed strategies to mitigate methane emissions from wetlands.

Data Availability: The metagenomic reads, metatranscriptomic reads, bacterial and archaeal MAGs, and 16S rRNA gene sequencing reads reported here have been deposited in the National Center for Biotechnology Information (**Supplementary Table S1**). To facilitate data accessibility, the 2,502 MAGs contained in this dataset, here identified as MUCC (Multi-omics to understand Climate Change) v.1 are publicly available as a KBase data collection, offering genomes and annotations for use in an accessible cyberinfrastructure powered platform with the intent to advance wetland science broadly (***https://narrative.kbase.us/narrative/147022***). Flux and meteorological observations for OWC are available through Ameriflux, Site ID US-OWC (19). Porewater methane concentrations and chamber fluxes are available through ESS-DiVE (18) and (44). Data for nutrient and carbon sequestration and soil accretion rates of OWC is available through ESS-DiVE (45). Additional meteorological, hydrological and water quality data for OWC is available through the NERR data system (https://cdmo.baruch.sc.edu/). LC-MS data is available through MassIVE under accession MSV000093935. Additionally, all MAGs, and derived gene calls, annotations, phylogenetic trees, and metatranscriptome abundance profiles are available on Zenodo DOI 10.5281/zenodo.8194032.

References

1. S. C. Neubauer, J. P. Megonigal, Moving Beyond Global Warming Potentials to Quantify the Climatic Role of Ecosystems. *Ecosystems* **18**, 1000–1013 (2015).

2. R. B. Jackson, *et al.*, Increasing anthropogenic methane emissions arise equally from agricultural and fossil fuel sources. *Environ. Res. Lett.* **15**, 071002 (2020).

3. S. D. Bridgham, H. Cadillo-Quiroz, J. K. Keller, Q. Zhuang, Methane emissions from wetlands: biogeochemical, microbial, and modeling perspectives from local to global scales. *Glob Chang Biol* **19**, 1325–1346 (2013).

4. K. Calvin, *et al.*, "IPCC, 2023: Climate Change 2023: Synthesis Report. Contribution of Working Groups I, II and III to the Sixth Assessment Report of the Intergovernmental Panel on Climate Change [Core Writing Team, H. Lee and J. Romero (eds.)]. IPCC, Geneva, Switzerland.," First (Intergovernmental Panel on Climate Change (IPCC), 2023).

5. R. Conrad, Importance of hydrogenotrophic, aceticlastic and methylotrophic methanogenesis for methane production in terrestrial, aquatic and other anoxic environments: A mini review. *Pedosphere* **30**, 25–39 (2020).

6. W. J. Riley, *et al.*, Barriers to predicting changes in global terrestrial methane fluxes: analyses using CLM4Me, a methane biogeochemistry model integrated in CESM. *Biogeosciences* **8**, 1925–1953 (2011).

7. B. Kieft, *et al.*, Genome-resolved correlation mapping links microbial community structure to metabolic interactions driving methane production from wastewater. *Nat Commun* **14**, 5380 (2023).

8. L. M. Solden, *et al.*, Interspecies cross-feeding orchestrates carbon degradation in the rumen ecosystem. *Nat Microbiol* **3**, 1274–1284 (2018).

9. M. A. Borton, *et al.*, Coupled laboratory and field investigations resolve microbial interactions that underpin persistence in hydraulically fractured shales. *Proceedings of the National Academy of Sciences* **115**, E6585–E6594 (2018).

10. N. Taş, *et al.*, Landscape topography structures the soil microbiome in arctic polygonal tundra. *Nat Commun* **9**, 777 (2018).

11. B. J. Woodcroft, *et al.*, Genome-centric view of carbon processing in thawing permafrost. *Nature* **560**, 49–54 (2018).

12. J. Hultman, *et al.*, Multi-omics of permafrost, active layer and thermokarst bog soil microbiomes. *Nature* **521**, 208–212 (2015).

13. R. M. Wilson, *et al.*, Soil metabolome response to whole-ecosystem warming at the Spruce and Peatland Responses under Changing Environments experiment. *Proceedings of the National Academy of Sciences* **118**, e2004192118 (2021).

14. G. J. Smith, *et al.*, Members of the Genus Methylobacter Are Inferred To Account for the Majority of Aerobic Methane Oxidation in Oxic Soils from a Freshwater Wetland. *mBio* **9**, e00815-18.

15. J. C. Angle, *et al.*, Methanogenesis in oxygenated soils is a substantial fraction of wetland methane emissions. *Nat Commun* **8**, 1567 (2017).

16. A. B. Narrowe, *et al.*, Uncovering the Diversity and Activity of Methylotrophic Methanogens in Freshwater Wetland Soils. *mSystems* **4**, e00320-19 (2019).

17. M. Bahram, *et al.*, Structure and function of the soil microbiome underlying N2O emissions from global wetlands. *Nat Commun* **13**, 1430 (2022).

18. G. Bohrer, *et al.*, Methane and CO2 chamber fluxes and porewater concentrations US-OWC Ameriflux wetland site, 2015-2018. Environmental System Science Data Infrastructure for a Virtual Ecosystem (ESS-DIVE) (United States); AmeriFlux Management Project. https://doi.org/10.15485/1568865. Deposited 1 October 2019.

19. G. Bohrer, J. Kerns, AmeriFlux BASE US-OWC Old Woman Creek. AmeriFlux AMP. https://doi.org/10.17190/AMF/1418679. Deposited 2023.

20. T. H. Morin, *et al.*, Water level changes in Lake Erie drive 21st century CO2 and CH4 fluxes from a coastal temperate wetland. *Science of The Total Environment* **821**, 153087 (2022).

21. E. J. Zakem, M. F. Polz, M. J. Follows, Redox-informed models of global biogeochemical cycles. *Nat Commun* **11**, 5680 (2020).

22. H. Chu, *et al.*, AmeriFlux BASE data pipeline to support network growth and data sharing. *Sci Data* **10**, 614 (2023).

23. G. Pastorello, *et al.*, The FLUXNET2015 dataset and the ONEFlux processing pipeline for eddy covariance data. *Sci Data* **7**, 225 (2020).

24. K. B. Delwiche, *et al.*, FLUXNET-CH4: a global, multi-ecosystem dataset and analysis of methane seasonality from freshwater wetlands. *Earth System Science Data* **13**, 3607–3689 (2021).

25. B. J. Baker, *et al.*, Genomic inference of the metabolism of cosmopolitan subsurface Archaea, Hadesarchaea. *Nat Microbiol* **1**, 1–9 (2016).

26. V. De Anda, *et al.*, Brockarchaeota, a novel archaeal phylum with unique and versatile carbon cycling pathways. *Nat Commun* **12**, 2404 (2021).

27. J. B. Ellenbogen, *et al.*, Methylotrophy in the Mire: direct and indirect routes for methane production in thawing permafrost. *mSystems* **0**, e00698-23 (2023).

28. M. S. M. Jetten, A. J. M. Stams, A. J. B. Zehnder, Methanogenesis from acetate: a comparison of the acetate metabolism in Methanothrix soehngenii and Methanosarcina spp. *FEMS Microbiology Letters* **88**, 181–197 (1992).

29. E. K. Bechtold, *et al.*, Metabolic interactions underpinning high methane fluxes across terrestrial freshwater wetlands. *Nat Commun* **16**, 944 (2025).

30. R. Conrad, Methane Production in Soil Environments—Anaerobic Biogeochemistry and Microbial Life between Flooding and Desiccation. *Microorganisms* **8**, 881 (2020).

31. M. J. Bogard, *et al.*, Oxic water column methanogenesis as a major component of aquatic CH4 fluxes. *Nat Commun* **5**, 5350 (2014).

32. H. Chen, *et al.*, Functional Redundancy in Soil Microbial Community Based on Metagenomics Across the Globe. *Front Microbiol* **13**, 878978 (2022).

33. S. M. Gibbons, *et al.*, Evidence for a persistent microbial seed bank throughout the global ocean. *Proceedings of the National Academy of Sciences* **110**, 4651–4655 (2013).

34. R. F. Grant, Simulation of methanogenesis in the mathematical model ecosys. *Soil Biology and Biochemistry* **30**, 883–896 (1998).

35. K. Wang, B. Xiong, X. Zhao, Could propionate formation be used to reduce enteric methane emission in ruminants? *Science of The Total Environment* **855**, 158867 (2023).

36. X. Xie, *et al.*, Mitigating enteric methane emissions: An overview of methanogenesis, inhibitors and future prospects. *Animal Nutrition* **21**, 84–96 (2025).

37. B. B. McGivern, *et al.*, Polyphenol rewiring of the microbiome reduces methane emissions. *The ISME Journal* wraf108 (2025). https://doi.org/10.1093/ismejo/wraf108.

38. I. Vanwonterghem, *et al.*, Methylotrophic methanogenesis discovered in the archaeal phylum Verstraetearchaeota. *Nat Microbiol* **1**, 1–9 (2016).

39. V. Krukenberg, A. J. Kohtz, Z. J. Jay, R. Hatzenpichler, Methyl-reducing methanogenesis by a thermophilic culture of Korarchaeia. *Nature* **632**, 1131–1136 (2024).

40. C. P. Bueno de Mesquita, D. Wu, S. G. Tringe, Methyl-Based Methanogenesis: an Ecological and Genomic Review. *Microbiology and Molecular Biology Reviews* **87**, e00024-22 (2023).

41. M. A. Borton, *et al.*, Comparative genomics and physiology of the genus Methanohalophilus, a prevalent methanogen in hydraulically fractured shale. *Environmental Microbiology* **20**, 4596–4611 (2018).

42. L. Y. Stein, M. E. Lidstrom, Greenhouse gas mitigation requires caution. *Science* **384**, 1068–1069 (2024).

43. Z. Li, *et al.*, A framework for integrating genomics, microbial traits, and ecosystem biogeochemistry. *Nat Commun* **16**, 2186 (2025).

44. E. Hassett, *et al.*, Carbon flux measurements from chambers collected between July to October 2022 at Old Woman Creek, Huron, Ohio. urn:node:ESS_DIVE. https://doi.org/10.15485/2229438. Deposited 2023.

45. J. Villa, G. Bohrer, L. Kinsman-Costello, Y. Ju, Nutrient and carbon concentrations in dated soil cores at US-OWC Ameriflux wetland site (OWC NERR). urn:node:ESS_DIVE. https://doi.org/10.15485/1839288. Deposited 2022.

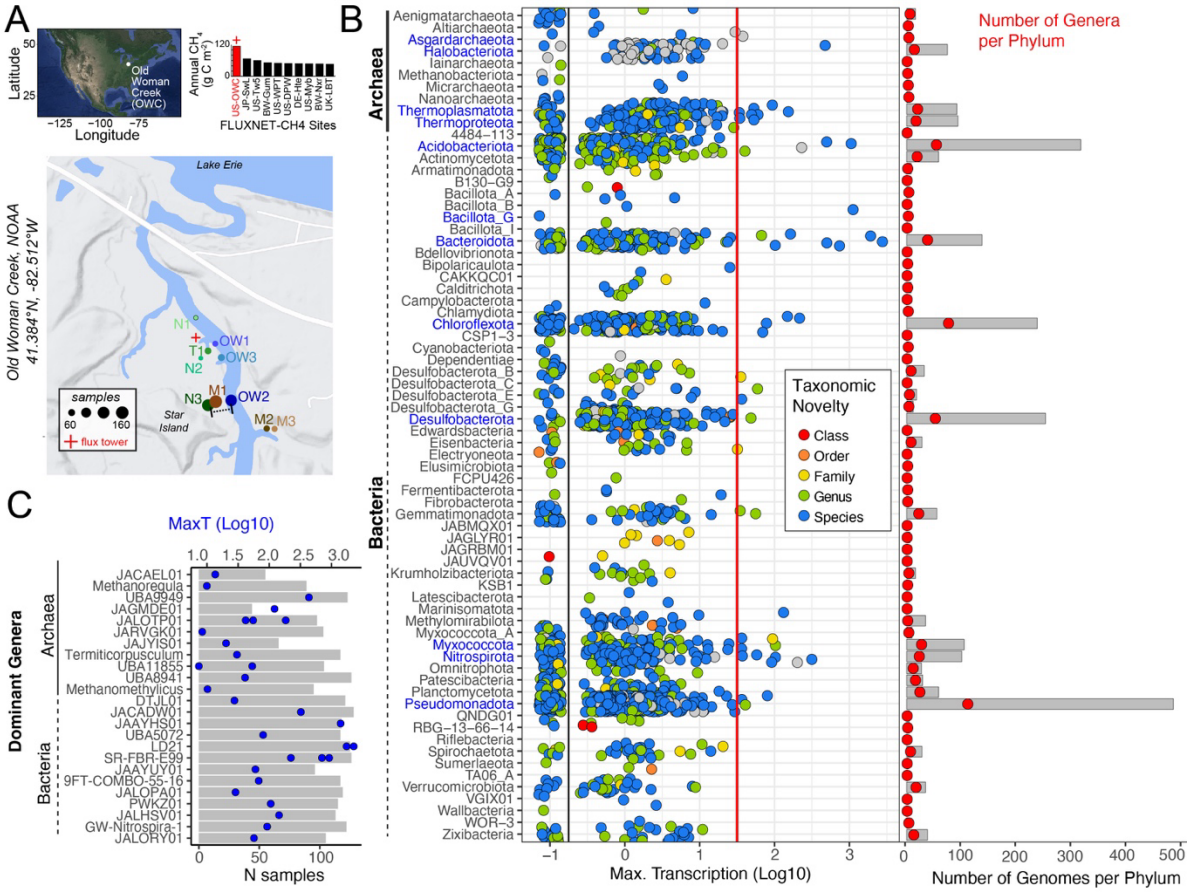

Figure 1. Freshwater wetland soils host thousands of taxonomically diverse MAGs that recruit metatranscripts. (A) Old Woman Creek (OWC) is located on the southern part of Lake Erie and is the highest US methane emitting wetland in the AmeriFlux Network. A site map of the OWC freshwater wetland shows where the 700 samples were collected from 10 major sampling sites that were historically

defined as emergent vegetation, either *Nelumbo* (N1-3) or *Typha* (T1), mud cover (M1-3), or location in open water channel (OW1-3). Sites were sampled over multiple years and depths at 5 cm intervals from 0-30 cm, with sampling density proportional to circle size, 52 is the minimum sampling per location (**Supplementary Fig. S1**). **(B)** The taxonomic distribution of the 2,502 MAGs summarized at the phylum level. Bold phylum label indicates a candidate phylum, and blue text indicates the phylum contains a top 12 dominant genus (shown in **1C**). Each point represents a MAG and is colored by taxonomic novelty. Points are distributed by their log10 maximum transcription across the 133 metatranscriptome samples. MAGs to the right of the black line were considered positive for sufficient transcript recruitment (N = 1,948). MAGs to the right of the red line had the greatest transcription (log10 max. transcription > 1.5). The gray bar chart to the right summarizes the number of genomes per phylum recovered, and red points overlaid represent the number of genera recovered within each phylum, using the same x-axis. **(C)** The transcriptionally most dominant archaeal and bacterial MAGs (top 12 for each domain) from 1B, grouped by genus. Gray bar indicates metatranscriptome prevalence (gray bar), or the number (N) of the 133 samples where metatranscripts were recruited to the MAG for that genus. The axis is shown on bottom (N samples). The blue dot indicates the maximum transcription from **1B**, with the axis (MaxT, Log10) shown at the top of the graph.

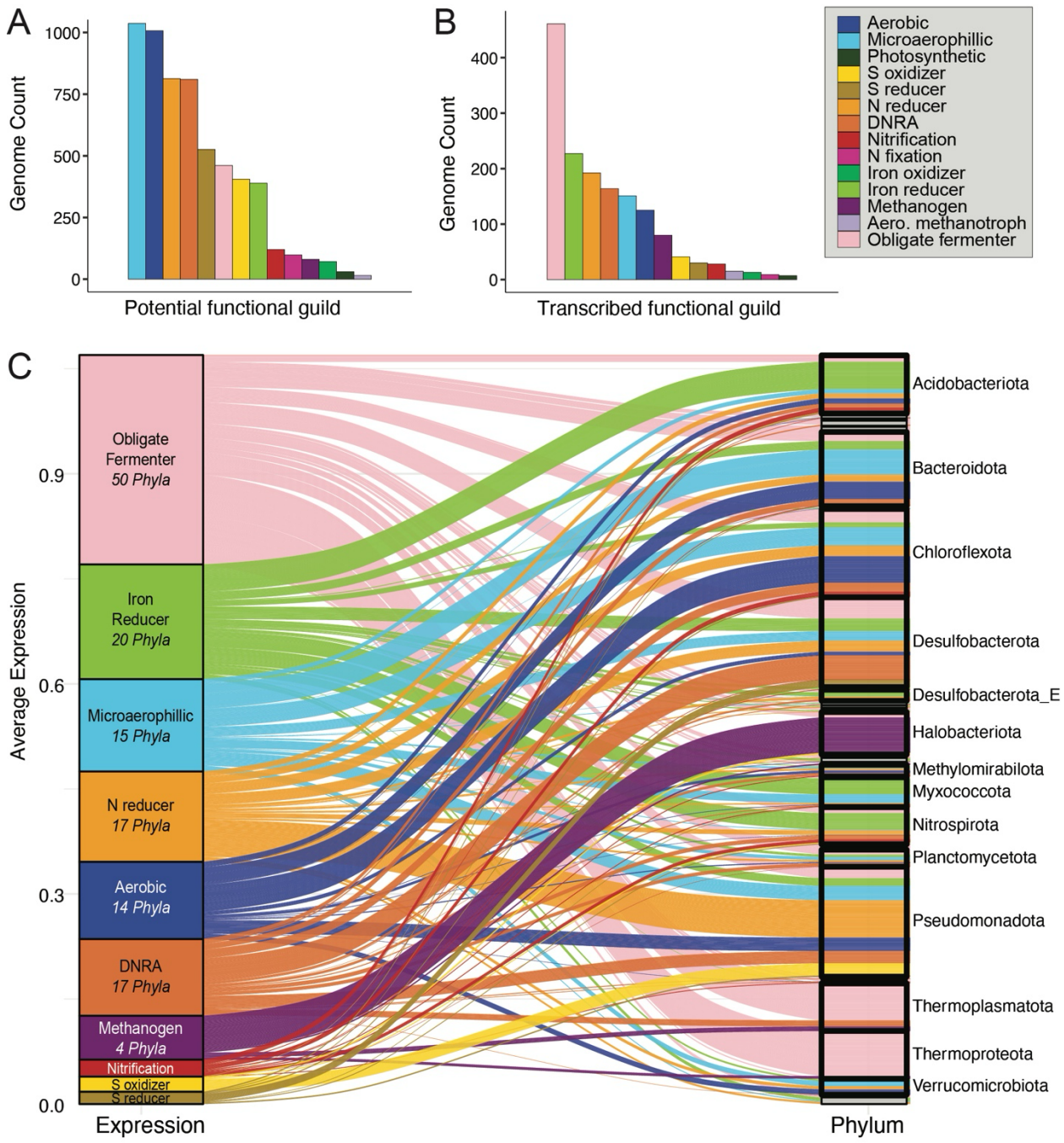

Figure 2. Distinct functional potential and expression across wetland microbial genomes. Bar plots summarize the genome counts across functional traits for genomic potential **(A)** and transcription **(B)**, respectively. **(C)** Alluvial plot illustrates the distribution of top 10 expressed metabolic guilds (left) and their corresponding phyla (right). The height of each flow represents the average expression of that metabolic guild in a particular phylum, with colors indicating different metabolic guilds. Labels for phyla with less than 0.01 total expression were omitted. Number of phyla for each guild is noted for 7 of top 10 phyla, with Nitrification (n=11 Phyla), S oxidizer (n=4 Phyla), and S reducer (n=7 Phyla) guilds detailed here.

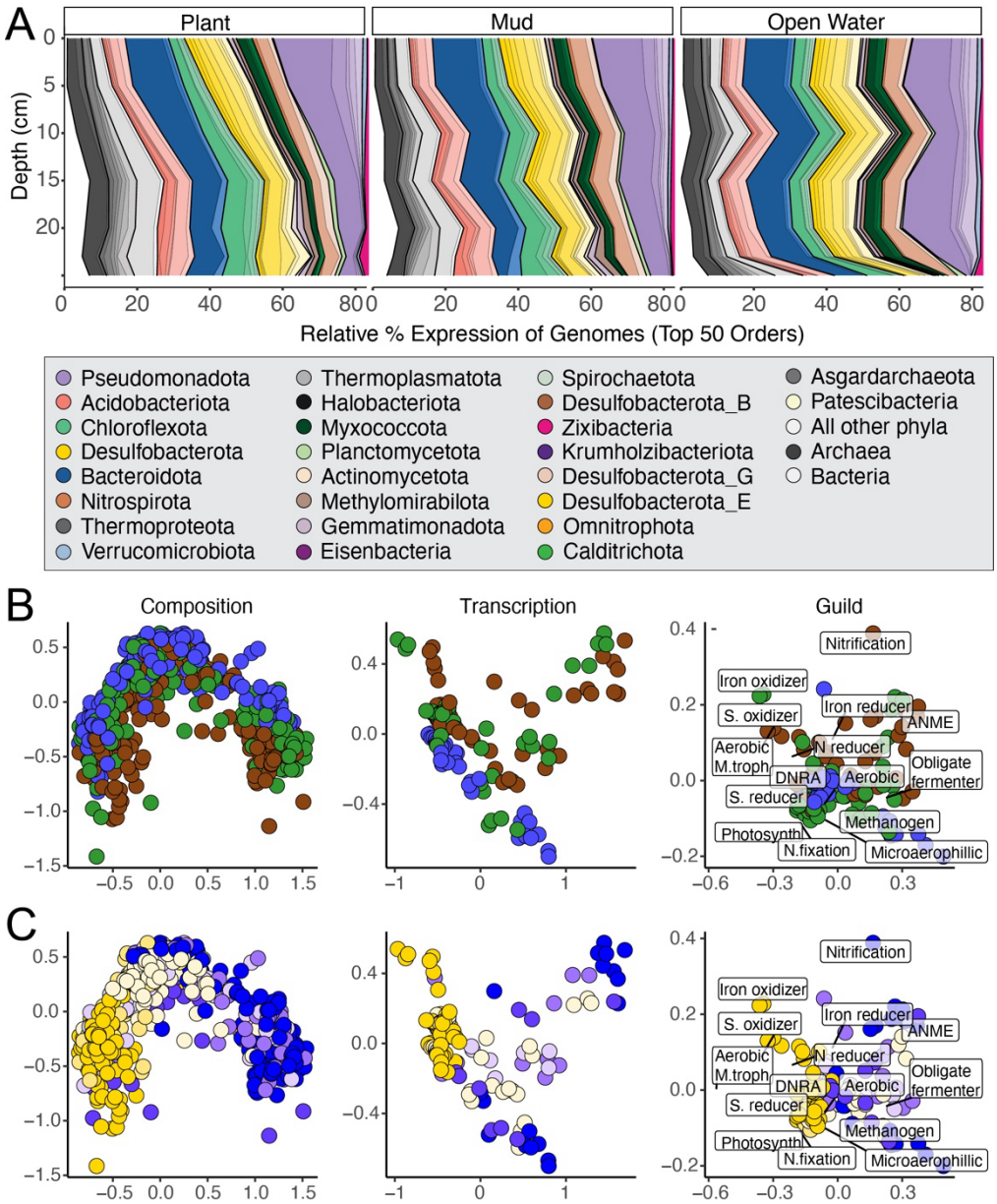

Figure 3. Depth structures wetland soil microbiomes. (A) Smoothed density plots for the top 50 orders, shaded by phylum level colors provided in the legend. Changes in the relative expression across the sampled depth gradient and across land coverage types (vegetative, mud, and open water). **(B-C)** Nonmetric multidimensional scaling (NMDS) ordinations of wetland microbiome structural metrics are organized from (left) overall composition (N=671), (middle) genome transcription (N=133), and (right) guild transcription (N=133).The samples are colored by land coverage in (**B**) (brown=mud; green=vegetative; blue=open water), while **(C)** is colored by depth (yellow=surface to blue=deep). B and C highlight the responses of the two major environmental predictors with depth being the strongest predictor across all soil microbiome attributes (**Supplementary Figure S4**).

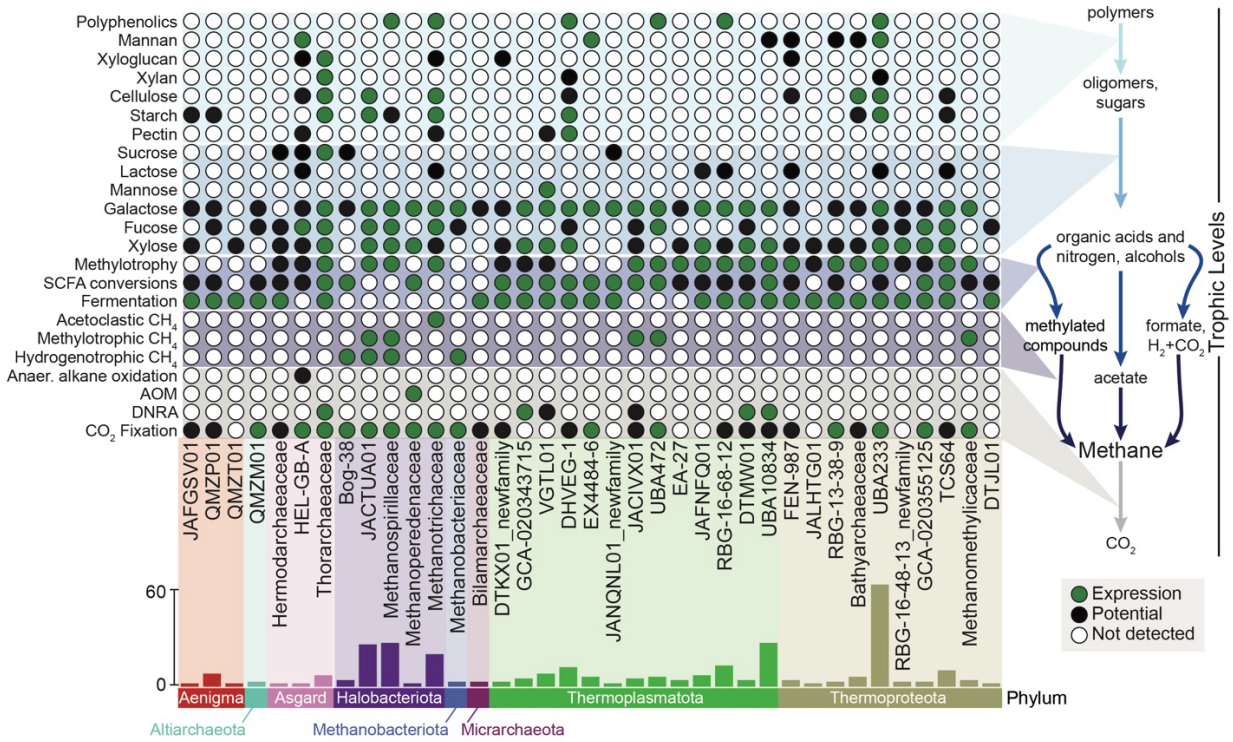

Figure 4. Assigning Archaeal roles in the wetland carbon cycle. (**Right**) The schematic on the right visualizes the major trophic levels contributing to soil carbon decomposition including: light blue polymers (polyphenolics, mannan, xyloglucan, xylan, cellulose, starch, pectin); medium blue oligomers and sugars (sucrose, lactose, mannose, galactose, fucose, xylose); dark blue organic acids, nitrogen, and alcohols (fermentation, methylotrophy, anaerobic alkane oxidation); purple methanogenesis (acetoclastic, methylotrophic, and hydrogenotrophic); and grey other 1 carbon metabolisms (anaerobic methane oxidation, CO_2 fixation). (**Left**) For each archaeal family the bubble plot denotes genes transcribed (green), genes present (black), or genes absent (white) for the major carbon utilization pathways assigned to the trophic levels. (**Bottom**) The bar chart summarizes the number of transcriptionally active MAGs recovered within each archaeal phylum and family.

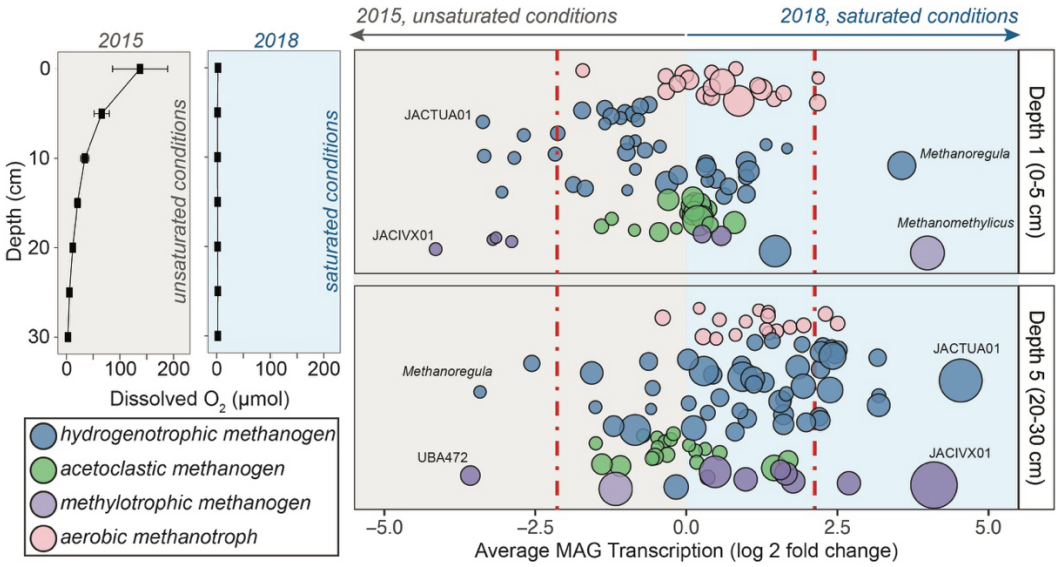

Figure 5. Methanogen stability in response to flooding. Dissolved porewater oxygen depth profiles from August 2015 (grey) and 2018 (blue) highlight the redox impact of flooding. Scatterplot shows the change of mean MAG transcription from 2015 to 2018 from the methane cycling community within surface (0-5 centimeters) and deep (20-30 centimeters) soil compartments. Bubbles represent a single methane cycling MAG and are colored by metabolism and sized by mean transcription. MAGs within the red dashed lines do not have log2 fold change in mean transcription and are considered temporally stable.

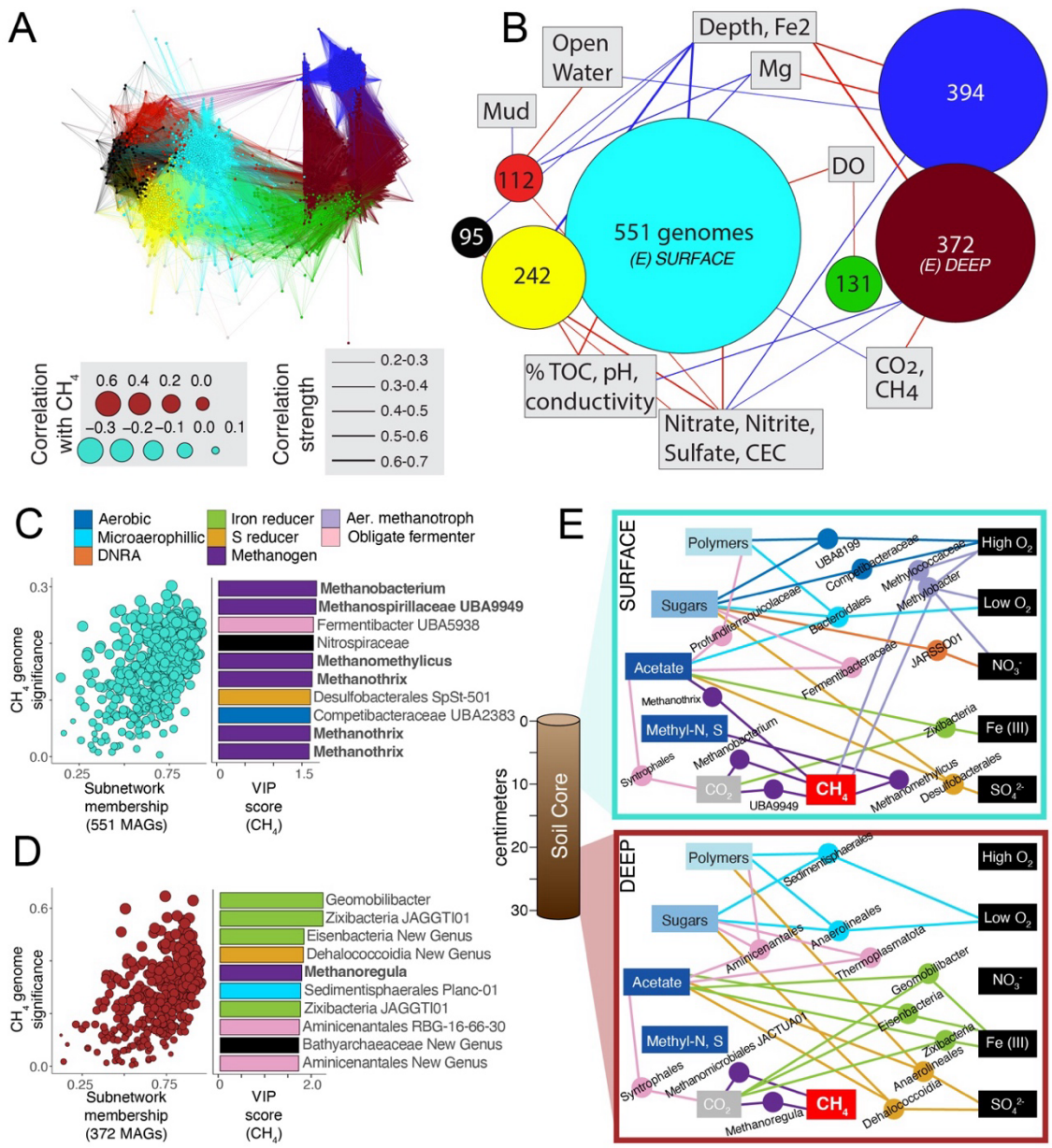

Figure 6. Coordinated gene expression networks predict wetland methane concentrations. **(A)** Overall co-expression network from 1,948 MAGs across 132 metatranscriptomics samples. Node outline colors highlight modules (where N > 100) identified with weighted gene co-expression analyses. **(B)** A simplified network diagram highlighting the associations between modules (sized scaled by number of MAGs) and environmental features. Red and blue edges correspond to positive and negative associations, respectively. **(C)** The genome significance plot and highest variable important genomes related to CH_4 concentrations in the turquoise, surface derived subnetwork (n = 551 MAGs, Rho = 0.53, P < 0.001). **(D)** The genome significance plot and highest variable important genomes related to CH_4 concentrations from the brown, deep subnetwork (n = 372 MAGs, Rho = 0.58, P < 0.001). For panels C and D, the bar charts (middle) highlight the relative contribution of the top 10 variably important genomes (colored by metabolic classification). Methanogens are highlighted with bold text. **(E)** A process-based schematic based on genome-resolved transcript data of the significant variable important projection (VIP, >1) taxa and their contribution to methane production in the surface subnetwork from A (top) and the deep subnetwork from B (bottom).